exists regarding the solution construction within the Grad – Shafranov equation method. The point is that the location of singular surfaces, at which critical conditions should be formulated, is not known beforehand and itself must be found from the solution to the problem. Moreover, it is impossible to generalize this approach to the case of nonideal, nonaxially symmetric and nonsteady flows. So it is not surprising that most investigators, who are primarily interested in astrophysical applications, have recently focused on a totally different class of equations, namely, on time relaxation problems, which can only be solved numerically [19]. Here, we would only like to hope that the key physical results obtained using the Grad – Shafranov equation, which, naturally, are independent of the computing method, are not forgotten.

References

1. Shapiro S, Teukolsky S A *Black Holes, White Dwarfs, and Neutron Stars* (New York: Wiley, 1983) [Translated into Russian (Moscow: Mir, 1985)]
2. Thorne K S, Price R H, MacDonald D A (Eds) *Black Holes*: *The Membrane Paradigm* (New Haven: Yale Univ. Press, 1986) [Translated into Russian (Moscow: Mir, 1988)]
3. Guderley K G *Theorie Schallnaher Stömungen* (Berlin: Springer, 1957) [Translated into English: *The Theory of Transonic Flow* (Oxford: Pergamon Press, 1962); Translated into Russian (Moscow: IL, 1960)]; von Mises R *Mathematical Theory of Compressible Fluid Flow* (New York: Academic Press, 1958) [Translated into Russian (Moscow: IL, 1961)]; Frankl' F I *Izbrannye Trudy po Gazovoĭ Dinamike* (Selected Works on Gas Dynamics) (Moscow: Nauka, 1973)
4. Shafranov V D *Zh. Eksp. Teor. Fiz.* **33** 710 (1957) [*Sov. Phys. JETP* **6** 545 (1958)]; Grad H *Rev. Mod. Phys.* **32** 830 (1960)
5. Solov'ev L S, in *Voprosy Teorii Plazmy* (Problems of Plasma Theory) Vol. 3 (Ed. M A Leontovich) (Moscow: Atomizdat, 1963) p. 245
6. Heinemann M, Olbert S *J. Geophys. Res.* **83** 2457 (1978); Okamoto I *Mon. Not. R. Astron. Soc.* **173** 357 (1975); Nitta S, Takahashi M, Tomimatsu A *Phys. Rev. D* **44** 2295 (1991)
7. Beskin V S, Par'ev V I *Usp. Fiz. Nauk* **163** (6) 95 (1993) [*Phys. Usp.* **36** 529 (1993)]
8. Beskin V S, Pidoprygora Yu N *Zh. Eksp. Teor. Fiz.* **107** 1025 (1995) [*JETP* **80** 575 (1995)]
9. Beskin V S *Usp. Fiz. Nauk* **167** 689 (1997) [*Phys. Usp.* **40** 659 (1997)]
10. Hunt R *Mon. Not. R. Astron. Soc.* **188** 83 (1979)
11. Beskin V S, Kompaneets R Yu, Tchekhovskoy A D *Pis'ma Astron. Zh.* **28** 616 (2002) [*Astron. Rep.* **28** 543 (2002)]
12. Shakura N I *Astron. Zh.* **49** 921 (1972) [*Sov. Astron.* **16** 756 (1973)]; Shakura N I, Sunyaev R A *Astron. Astrophys.* **24** 337 (1973); Novikov I D, Thorne K S, in *Black Holes* (Eds C DeWitt, B S DeWitt) (New York: Gordon and Breach, 1973) p. 343
13. Paczynski B, Bisnovatyi-Kogan G *Acta Astron.* **31** 283 (1981)
14. Blandford R D, Znajek R L *Mon. Not. R. Astron. Soc.* **179** 433 (1977)
15. Beskin V S *Usp. Fiz. Nauk* **169** 1169 (1999) [*Phys. Usp.* **42** 1071 (1999)]
16. Punsly B, Coroniti F V *Astrophys. J.* **350** 518 (1990)
17. Beskin V S, Kuznetsova I V *Nuovo Cimento B* **115** 795 (2000); astro-ph/0004021
18. Livio M, Ogilvie G I, Pringle J E *Astrophys. J.* **512** 100 (1999); Ghosh P, Abramowicz M A *Mon. Not. R. Astron. Soc.* **292** 887 (1997)
19. Hawley J F, Wilson J R, Smarr L L *Astrophys. J.* **277** 296 (1984); Petrich L I et al. *Astrophys. J.* **336** 313 (1989); Ustyugova G V et al. *Astrophys. J.* **439** L39 (1995); Koide S et al. *Astrophys. J.* **536** 668 (2000)

PACS numbers: **42.50.–p**, 42.50.Hz, **42.65–k**
DOI: 10.1070/PU2003v046n11ABEH001662

Coherent light scattering stimulated by a quasi-static electric field

V N Ochkin, S N Tskhaĭ

1. Introduction

This work concerns radiation arising from the dipole-forbidden molecular transition in the case of nondegenerate four-wave interaction. One wave being unrelated to light emission, its frequency is zero or close to zero. Parallel monitoring of scattering intensity and anti-Stokes signal intensities during a degenerate CARS process provides for the absolute measurement of the static field strength, while polarization measurements permit us to determine its direction. Due to the coherent and multiphoton nature of the scattering process, the application of this approach, unlike other known methods of Stark spectroscopy, makes it possible to measure field characteristics in gases and plasma under elevated pressure. In what follows, we give examples of measurement in gas discharges.

In the presence of an electric field in an isotropic medium for centrally symmetric particles, the selection rules for dipole transitions can vary. E Condon [1] was the first to demonstrate as early as 1932 that the description of such transitions may be analogous to the description of Raman scattering of light at a scattered wave frequency tending to zero (constant field). Later on, spectroscopic constants were calculated more precisely based on the measurements of electric field-induced absorption of infrared (IR) radiation by homonuclear molecules H_2, D_2, and N_2 [2–5].

Progress in laser technology and nonlinear optics gave rise to many works on the generation of coherent harmonic and mixed-frequency radiation, including generation in an external electric field that permits us to ease the alternative forbidding. Early studies [6–8] have helped to elucidate the generation of radiation at the difference frequency during stimulated Raman scattering (SRS) of light from ruby and neodymium lasers in H_2 in an electric field. SRS is known to have a high transformation threshold; in experiments [6, 7], generation of radiation occurred at hydrogen pressure $p > 5.5$ atm. This and the fact that the limitation on the spectrum is only imposed by strongest transitions make it very difficult to use SRS for quantitative measurements.

This paper reports studies on electric field-induced IR radiation in hydrogen using biharmonic pumping of vibrational transition and the application of this radiation to measuring field parameters, in particular, for the diagnostics of gas-discharge plasma.

2. Method. Experimental technique

We shall consider electric field-induced transitions as proposed by Condon [1], i.e., by analogy with the well-developed scheme of coherent anti-Stokes Raman scattering (CARS) (see, for instance, monograph [9]). Figure 1 represents schematically degenerate (a) and nondegenerate (b) CARS transitions along with coherent IR transition (c) induced by field $E(\omega = 0)$. In CARS spectroscopy, biharmonic pumping by two waves of laser light ω_1 and ω_2 (such that the frequency difference $\omega_1 - \omega_2 = \Omega$ corresponds to the frequency of

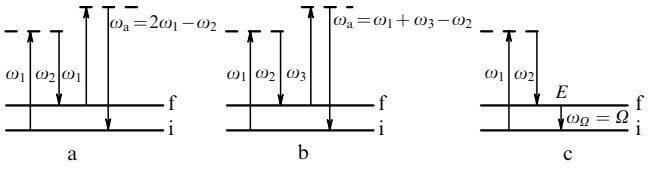

Figure 1. Schematics of degenerate (a) and nondegenerate (b) CARS transitions and generation of IR radiation in the presence of an electric field (c).

Raman-active molecular transition i → f) results in resonance excitation of coherent molecular vibrations from which one of the waves is scattered (the wave with frequency ω_1 in Fig. 1a). Evidently, the scattered wave may be of a different frequency (nondegenerate CARS, $\omega_3 \neq \omega_1$, Fig. 1b). We are interested in a limiting case with $\omega_3 = 0$ (constant electrical field, Fig. 1c).

Degenerate CARS intensity is described by the expression [9]

$$I_{\mathrm{CARS}} \sim \left| \chi^{(3)}_{\mathrm{CARS}} \right| I_1^2 I_2 \,, \qquad (1)$$

where $\chi^{(3)}$ is the third-order susceptibility, while I_1 and I_2 are laser beam intensities.

To continue the analogy with the traditional phenomenological CARS scenario, the intensity of E field-induced radiation under biharmonic pumping can be presented in the form [10]

$$I_\Omega \sim \left| \chi^{(3)}_\Omega \right|^2 I_1 I_2 E^2 \,. \qquad (2)$$

The physical sense of generation of IR radiation is rather simple. In the absence of a field, the transition is parity-forbidden; in its presence, the combining states 'mix in' with electronic states of a different parity [11].

This relationship was experimentally verified using an installation based on a standard CARS spectrometer as described in Refs [12, 13]. An Nd:YAG laser with a wavelength of 1.06 μm, pulse-repetition frequency 20 Hz, and pulse duration 10 ns served as the master generator, while radiation of the second harmonic $\lambda = 532$ nm represented the reference signal (wave ω_1). The spectral line width was 0.2 cm^{-1}, beam diameter 7 mm, and pulse energy 40 mJ. The same radiation was utilized to pump a dye laser in which a mixture of pyridine-1 and DCM dissolved in dimethylsulfoxide (DMSO) was made to cause lasing at $\lambda = 683$ nm (wave ω_2) with a pulse energy of 3 mJ. The width of laser line was 0.2 cm^{-1}, and the beam 2.5 mm in diameter.

Frequency difference $\omega_1 - \omega_2 = \Omega$ corresponded to the frequency of Raman-active vibrational–rotational transition Q(1) of the hydrogen molecule ($v = 0$, $J = 1 \rightarrow v = 1$, $J = 1$) in the ground electronic state $X^1\Sigma_g^+$ ($\lambda = 2.41$ μm).

Beams ω_1 and ω_2 were superimposed collinearly with the aid of dichroic mirrors and focused onto the object under study. The direction of linear polarization of the laser light was controlled and could be varied. In calibration experiments, the directions of the constant field (2.5–4 kV cm^{-1}) and laser beam fields were parallel. Hydrogen pressure ranged from 1 to 10 atm.

The IR signal of coherent Raman scattering generated in the cuvette was separated from the pumping beams ω_1 and ω_2 and from higher orders of coherent Stokes scattering by means of the system of filters.

IR radiation was recorded with a cooled InSb detector. The detected signal was accumulated, averaged using a BOXCAR integrator, and registered on a recorder. In order to detect a CARS signal, a mirror was introduced into the light beam to deflect radiation toward the photoelectric multiplier. In another experimental run, the up-conversion scheme was employed, in which the infrared light merged with pumping wave ω_1 in a $LiNbO_3$ crystal, and the radiation with a wavelength of 435 nm was recorded by the photomultiplier.

Direct detection of coherent IR radiation permitted the recording of an electric field strength as small as 50 V cm^{-1} at a hydrogen pressure of 1 atm, compared with 20 V cm^{-1} using the up-conversion technique. In either case, the sensitivity of detection was limited by the electrical noise from Nd : YAG laser power supply.

According to expression (2), the IR signal amplitude shows linear dependence on pump wave intensities, and quadratic dependence on the constant electric field strength. Strong biharmonic pumping may give rise to processes related to the motion of level populations that tend to distort these dependences. Additional experiments were undertaken to be convinced of the lack of such nonlinearities. The laser radiation power was varied employing neutral light filters and monitored with the aid of an IMO-2N power meter. Testing measurements demonstrated that the dependences in hand were well-described by expression (2) within experimental error.

Of primary importance is the fact that susceptibilities in Eqns (1) and (2) are the functions not only of polarization directions and frequencies (which it is easy to verify) but also of the populations of Raman levels i and f for IR transition. Field strength measurements give ambiguous results when N_i and N_f populations are unknown. It should be noted that this difficulty is intrinsic in all Raman scattering scenarios. By way of example, special measures are needed for traditional CARS to minimize particle redistribution between different levels under the effect of strong laser pumping. Population redistribution is characteristic of plasma conditions and chemical reactions, which is difficult to take into account in the absence of thermodynamic equilibrium. Fortunately, the measuring procedure under consideration permits us to overcome this problem due to the parallelism between the generation of IR radiation during dipole-forbidden transition and anti-Stokes radiation in the traditional degenerate CARS scenario. Because susceptibilities in relationships (1) and (2) show similar dependence on populations, viz. $\chi^{(3)} \propto (N_i - N_f)$, the intensity ratio $I_\Omega / I_{\mathrm{CARS}}$ depends only on the electric field strength squared and does not depend on the particle number density at levels i and f. It means that simultaneous recording of intensities I_Ω and I_{CARS} allows for the absolute measurement of the field strength even when strong biharmonic pumping or other factors induce population variations at the molecular vibrational levels. This is true on condition that the electric field nonuniformity has a characteristic scale larger than the spatial resolution of the measurements. It is worth noting, to illustrate the local character of the measurements, that the spatial resolution of the experimental setup used in the present study depended on the size of the laser beam waist and was approximately 0.1 mm transversely, and 1 mm along the beam path.

An alternating electric field of frequency ω can also function as field E. In this case, the IR radiation is generated at side frequencies $\omega_\Omega = \omega_1 - \omega_2 \pm \omega$, and its intensity is proportional to the square of the oscillating field amplitude.

3. Polarization properties

To study polarization properties of the electric field-induced coherent IR radiation, the experimental setup was equipped with polarizing elements, i.e., two Fresnel rhombi to rotate the plane of polarization of laser beams, and a Glan prism to serve as the analyzer [14].

A series of measurements were performed to determine the direction of field polarization in the cell at varying angles between the laser light's planes of polarization and the constant field direction.

Signal polarization in the case of nondegenerate four-wave mixing [9] is written as

$$\mathbf{P}_{\Omega}^{(3)}=6EE_1E_2\left[\chi_{1122}^{(3)}\mathbf{e}(\mathbf{e}_1\mathbf{e}_2^*)+\chi_{1212}^{(3)}\mathbf{e}_1(\mathbf{e}\mathbf{e}_2^*)+\chi_{1221}^{(3)}\mathbf{e}_2^*(\mathbf{e}\mathbf{e}_1)\right], \tag{3}$$

where E, E_1, and E_2 are field strengths, $\mathbf{e}$, $\mathbf{e}_1$, and $\mathbf{e}_2$ are unit vectors showing directions of the constant field and pumping waves ω_1 and ω_2, respectively, and χ_{ijkl} are the components of the nonlinear susceptibility tensor. Susceptibilities $\chi^{(3)}$ in formulas (1) and (2) are the tensors of fourth rank with the 81 components. However, only three of them are independent because of isotropic medium symmetry: $\chi_{1111}=\chi_{1122}+\chi_{1212}+\chi_{1221}$. For totally symmetrical vibrations, specifically for an H_2 molecule in the ground electronic state, one has $\chi_{1212}^{(3)}=\chi_{1221}^{(3)}$. In this case, only two independent components of the nonlinear susceptibility tensor will be left over. It follows from formula (3) that the signal has maximum intensity, when polarizations of all the three fields are parallel. By rotating the plane of polarization of one pumping wave, e.g., ω_1, and retaining that of the other (ω_2) parallel to the constant field, it is possible to determine all components of the susceptibility tensor.

Intensity measurements of the hydrogen transition under investigation at two directions ($\mathbf{e}\|\mathbf{e}_2\perp\mathbf{e}_1$ and $\mathbf{e}\|\mathbf{e}_2\|\mathbf{e}_1$) of polarization can be used to determine the ratio of the components of the nonlinear susceptibility tensor [14, 15]:

$$\frac{\chi_{1122}^{(3)}}{\chi_{1212}^{(3)}}=17.3\pm2.1\,. \tag{4}$$

This value is in good agreement with the values of Raman scattering tensor invariants — mean polarizability $\alpha_{01}=1.04\times10^{-25}$ cm^3 and anisotropy $\gamma_{01}=0.794\times10^{-25}$ cm^3 measured from the radiation absorption on the same transition in hydrogen in the presence of an external electric field [2] — in correspondence with the known relations that connect these invariants with the components of the nonlinear susceptibility tensor [9].

For collinear vectors of polarization ($\mathbf{e}_1\|\mathbf{e}_2$) of pumping waves, the signal polarization vector can be represented in the form

$$\mathbf{P}_{\Omega}^{(3)}=6EE_1E_2\left(\chi_{1122}^{(3)}\mathbf{e}+2\chi_{1212}^{(3)}\mathbf{e}_1\cos\varphi\right),$$

where φ is the angle between the constant field vector $\mathbf{e}$ and the vectors of polarization $\mathbf{e}_1\|\mathbf{e}_2^*$ of pumping waves. Therefore, given the direction of polarization of the IR signal, the opportunity knocks for deducing the orientation of the constant electric field. Different measuring procedures can be utilized for the purpose [14]. For example, having $\mathbf{e}_1\|\mathbf{e}_2$ and knowing the direction of the electric field vector $\mathbf{E}$, it is possible to plot the angle α between IR signal polarization vectors and the field vector against the angle φ between collinear laser polarization vectors and the field vector (Fig. 2). Measurement of IR signal polarization with an analyzer placed in front of the radiation detector permits us to determine the direction of the electric field strength vector directly from the plot. For a hydrogen molecule, deflections of the IR polarization vector from the vector of the constant electric field are small; the same ensues from formula (4) ($\chi_{1122}^{(3)}/\chi_{1212}^{(3)}\gg1$). The calculated deflections at the measured values of the nonlinear susceptibility tensor are represented in Fig. 2 as a solid line. The maximum deflection amounts to $\sim3^\circ$.

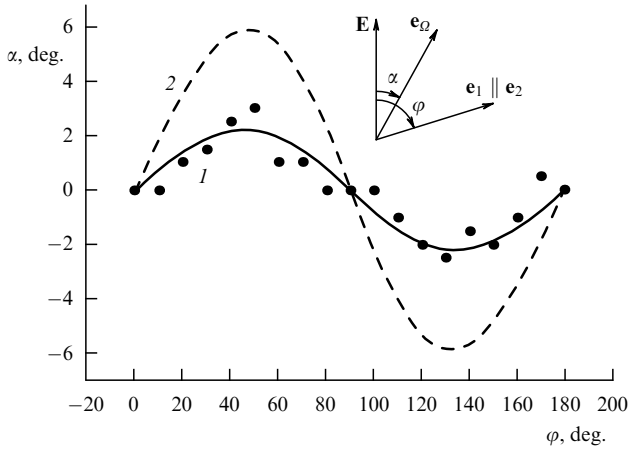

Figure 2. Angle of deflection of IR signal polarization vector from the direction of constant electrical field as a function of the angle between collinear vectors of pump waves and field vector. *1* — calculation for H_2 molecule, *2* — calculation for N_2, circles — experimental values for H_2.

If the components of the nonlinear susceptibility tensor are known, then the dependence depicted in Fig. 2 may be computed. By way of example, Fig. 2 shows the theoretical curve for a nitrogen molecule calculated from the invariants of the Raman scattering tensor borrowed from Ref [4].

It follows from formula (3) that for $\mathbf{e}_1\|\mathbf{e}_2\|\mathbf{e}$ or $\mathbf{e}_1\|\mathbf{e}_2\perp\mathbf{e}$, polarization of the IR signal is $\mathbf{e}_\Omega\|\mathbf{e}$ (see Fig. 2). To conclude, by performing two measurements for laser polarizations in two orthogonal planes, the opportunity appears to measure components of the electric field vector, the magnitudes of which will be determined through the IR signal intensity:

$$\sqrt{I_{\Omega\tau}}\propto\chi_{1111}E_\tau E_1E_2\,,\quad\sqrt{I_{\Omega n}}\propto\chi_{1122}E_nE_1E_2\,. \tag{5}$$

4. Coherent Stark spectroscopy of gas-discharge plasma

The electric field constitutes the major factor accounting for the existence of many types of gas discharges. In this case the spatial structures of gas-discharge plasma fields can be very complex. Naturally, the determination of internal field characteristics is an important part of their diagnostics. All known optical techniques make use of the Stark effect. The classical spectral methods concerned with radiation emission and absorption have essential limitations imposed by their sensitivity, number densities of neutral and charged particles, etc. (see, for instance, Ref. [16]). In recent years, this gave impetus for the development of new techniques with the use of lasers that can be tuned to a wide range of frequencies. Considerable progress was achieved in the application of

laser-induced fluorescence spectra formed with the participation of Rydberg states (in atoms) and Λ-doubled states (in molecules) [17 – 19]. However, these methods (like classical ones) are subject to stringent restrictions in terms of plasma-forming gas pressure (as a rule, from fractions of a torr to several torrs). Such limitations are due to incoherence of the previously used spectroscopic techniques that covered states with the finite radiative lifetime. Being sensitive to electric field effects (level splitting, appearance of 'forbidden' components), these schemes are equally sensitive to particle collisions in plasma.

In principle, the scattering discussed in the present paper results from the removal of the radiation forbidding; there is, however, an additional radical difference. In our case, the process is of a coherent and multiphoton nature, with the scattering particle being not fixed in intermediate states, and the role of collisions is significantly smaller. It has been shown in experiments that the relationship between the scattering intensity and the strength of the stimulating field (2) persists up to a few or tens of atmospheres [12].

For the above reasons, this method is naturally applied to the study of gas discharges under elevated pressure conditions. Relevant examples are given below.

4.1 Corona discharge

We have performed local measurements of the electric field strength in a positive corona discharge in hydrogen [12].

The discharge was drawn using 40 mm long coaxial cylindrical electrodes of radii $r_0 = 0.075$ mm and $r_1 = 8.5$ mm. Constant voltage $U = 7$ kV was maintained between the electrodes. Conditions for the existence of the corona discharge were determined by hydrogen pressure in the cuvette and monitored by measuring an electric current across the discharge gap. The corona discharge was absent at a hydrogen pressure of 10 atm. Figure 3 shows electrostatic radial distribution of the electric field strength derived from the Poisson equation (curve *1*). Under hydrogen pressure of 1.6 atm, the discharge current was $i_1 = 270$ μA. The distribution of the electric field strength in the corona was calculated by the well-known method described, for example, in Ref. [20] (Fig. 3, curve *2*). Circles in this figure show results of local measurements of the electric field strength, performed with the aid of the method proposed. It is clear from the foregoing that the discharge in question has been thoroughly investigated and employed as a model. There is excellent agreement between the experimental data and theoretical curves that demonstrates the high value of the method for measuring electric fields in real objects.

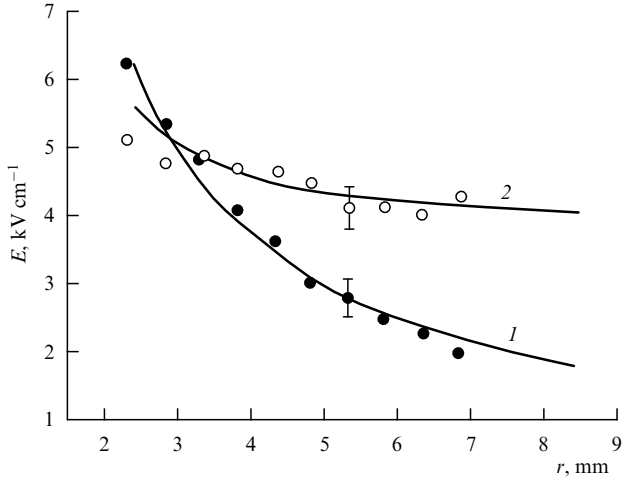

Figure 3. Distribution of the electric field strength in a corona discharge: *1* — calculation in the absence of discharge, *2* — calculation in the presence of discharge; circles — experimental values.

4.2 Sliding discharge on the ferrite surface

Discharge of this type is of interest for the development of light sources with high brightness temperature (~ 30 kK), operated (unlike exploding-wire light sources) in the frequency-dependent mode [13, 21]. One objective of our work was to study electric field dynamics during development of the discharge.

The discharge was drawn using a ferrite plate of 1×0.1 cm^2 cross-sectional area and 0.5 Ω^{-1} cm^{-1} conductivity (at an electric field strength of 1.5 kV cm^{-1}). The electrodes were attached to the narrow edge of the ferrite plate 4 – 12 mm from each other. Such a geometry allowed the discharge channel to be localized. Electrode voltage was varied from 1 to 3 kV. The plate was placed in a cuvette filled with molecular hydrogen at atmospheric pressure. The discharge-pulse repetition rate of 5 Hz was synchronized from the master-oscillator laser through the controlled delay line. Beams were brought together using collinear scheme and aligned perpendicularly to the discharge channel. They were focused ~ 1 mm above the ferrite surface. Polarization of the laser light was parallel to the direction of the discharge propagation.

As a voltage was applied, plasma channels propagated from the electrodes towards one another at significantly different velocities [21, 22]. The discharge glow was recorded with a photodiode placed opposite the discharge gap. The location of laser pulse glow enabled an accurate determination of the time delay of measurement with respect to the start of the discharge and plasma streamers closing (onset of intense discharge glow). The electric field strength was measured prior to the discharge onset and after its initiation till the plasma channels were closed. After the channel closing, the plasma column voltage dropped sharply and the electric field strength at the measuring point decreased below the threshold of sensitivity of the experimental setup.

Until the instant of commutation, a coherent IR signal is generated in the presence of an electrostatic field produced by the charged ferrite surface and electrodes to which an equal potential is applied. The electrostatic field depends on the charge at the ferrite surface. This signal was used for the adjustment of the system. Measurements of polarization confirmed that the direction of the electric field prior to the discharge onset was normal to the ferrite surface. After signal calibration, knowing the charging capacitor voltage it is possible to compute the distance between the measuring point and the ferrite surface.

After the discharge is switched on, one electrode is earthed and acquires zero potential, while the tangential component of the electric field strength is brought about in the discharge gap. By placing the polarization analyzer in front of the IR detector, the opportunity knocks for measuring dynamics of normal (with the polarizer perpendicular to the discharge axis) and tangential (with the polarizer parallel to the discharge axis) components of the electric field strength. The results of these measurements are presented in Figs 4a, b. Figure 4c also shows the angle of rotation of the polarization vector during the motion of plasma channels. The spacing between the

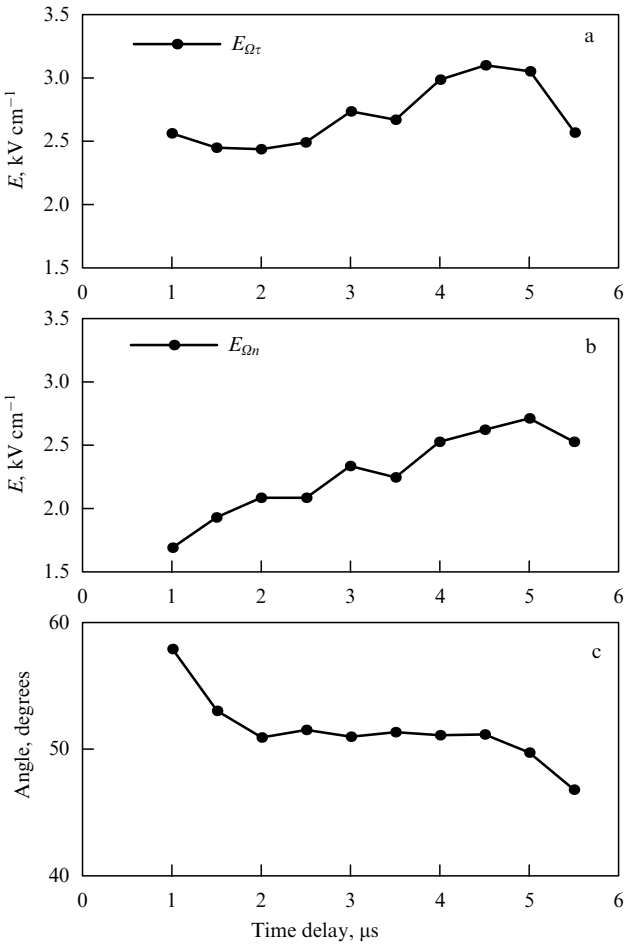

Figure 4. Dynamics of the electric field strength in a creeping discharge. (a,b) tangential and normal components of the electric field, respectively; (c) angle between the electric field vector and the discharge axis.

electrodes is 11 mm, the measuring point is located 3 mm from the anode and 1 mm above the ferrite surface.

The measurements were calibrated with respect to the tangential signal by means of its approximation to the instant of the discharge initiation, when the field strength was determined on the basis of high-voltage electrode readings and the electrode spacing. From the signal intensity ratio of parallel to perpendicular positions of the polarization analyzer (5) one can determine the normal component of the field strength. The normal and tangential components were compatible, and the electric field vector near the head of the plasma leader was inclined at an angle of 45° to the axis of the discharge (Fig. 4c).

The electric field strength was measured during development of the discharge sliding across the ferrite surface. Estimate of electron drift velocities corresponding to the measured strengths of the electric field indicated that they were close to the propagation velocity of the anode-directed streamer. This suggests a mechanism of discharge development mediated through direct ionization by electron impact near the channel head that serves as the virtual cathode.

5. Conclusion

Generation of IR radiation at the vibrational–rotational transitions of a centrosymmetrical molecule in a constant electrical field is a consequence of the eased alternative forbidding by virtue of the Stark effect. Light fields responsible for biharmonic excitation, static field with a zero wavenumber, and scattered radiation are the constituents of the process of the four-wave nondegenerate coherent interaction. This process may be used to generate coherent radiation for which the intrinsic gas is highly transparent. Also, it is possible to apply it, in conjunction with the known CARS schemes, to the absolute measurement of electric fields in gases and plasma with a high temporal and spatial resolution. The method is helpful at elevated gas pressure when other spectroscopic techniques are difficult to use.

This work was supported by the program "Optics and Laser Physics. Optical Spectroscopy and Frequency Standards" of the Division of Physical Sciences, RAS; Federal Target Program "Research and Development in Priority Areas of Science and Technology" (state contract 40.020.1.1.1157); Federal Target Program "Integration" (project B0049), NATO-Russia grant (No. 978204), and Russian Foundation for Basic Research (grant 02-02-81008).

References

1. Condon E U *Phys. Rev.* **41** 759 (1932)
2. Foltz J V, Rank D H, Wiggins T A *J. Mol. Spectrosc.* **21** 203 (1966)
3. Buijs H L, Gush H P *Can. J. Phys.* **49** 2366 (1971)
4. Courtois D, Jouve P *J. Mol. Spectrosc.* **55** 18 (1975)
5. Hunt R H, Barnes W L, Brannon P J *Phys. Rev. A* **1** 1570 (1970)
6. Butylkin V S et al. *Kvantovaya Elektron.* **2** 2282 (1975) [*Sov. J. Quantum Electron.* **5** 1242 (1975)]
7. Butylkin V S et al. *Rezonansnye Vzaimodeĭstviya Sveta s Veshchestvom* (Resonance Interactions of Light and Matter) (Moscow: Nauka, 1977) [Translated into English: *Resonant Nonlinear Interactions of Light with Matter* (Berlin: Springer-Verlag, 1989)]
8. Capasso F, De Martini F *Opt. Commun.* **9** 172 (1973)
9. Akhmanov S A, Koroteev N I *Metody Nelineĭnoĭ Optiki v Spektroskopii Rasseyaniya Sveta. Aktivnaya Spektroskopiya Rasseyaniya Sveta* (Methods of Non-Linear Optics in Scattered Light Spectroscopy. Active Scattered Light Spectroscopy) (Moscow: Nauka, 1981)
10. Gavrilenko V P et al. *Pis'ma Zh. Eksp. Teor. Fiz.* **56** 3 (1992) [*JETP Lett.* **56** 1 (1992)]
11. Sobel'man I I *Vvedenie v Teoriyu Atomnykh Spektrov* (Introduction to the Theory of Atomic Spectra) (Moscow: Nauka, 1977) [Translated into English (Oxford: Pergamon Press, 1972)]
12. Evsin O A et al. *Kvantovaya Elektron.* **22** 295 (1995) [*Quantum Electron.* **25** 278 (1995)]
13. Tskhai S N et al. *J. Raman Spectrosc.* **32** 177 (2001)
14. Akimov D A et al. *Pis'ma Zh. Eksp. Teor. Fiz.* **70** 371 (1999) [*JETP Lett.* **70** 375 (1999)]
15. Akimov D A et al., in *XVIII European CARS Workshop: CARS and Related Gas-Phase Laser Diagnostics, Frascati, Italy, March 21–23, 1999*, Book of Abstracts Vol. 85 (1999)
16. Ochkin V N et al. *IEEE Trans. Plasma Sci.* **PS-26** 1502 (1998)
17. Ochkin V N, Preobrazhensky N G, Shaparev N Ya *Optogalvanic Effect in Ionized Gas* (London: Lebedev Phys. Inst. Univ. Press, Found. for Intern. Sci. and Education Cooper.; Amsterdam: Gordon and Breach, 1999)
18. Ochkin V N et al. *Usp. Fiz. Nauk* **148** 473 (1986) [*Sov. Phys. Usp.* **29** 260 (1986)]
19. Ochkin V N, in *Entsiklopediya Nizkotemperaturnoĭ Plazmy* (Ed. V E Fortov) Vvodnyĭ Tom. Kn. 2 (Encyclopedia of Low-Temperature Plasma (Ed. V E Fortov) Introductory Volume. Book 2) (Moscow: Nauka, 2000) p. 411
20. von Engel A *Ionized Gases* (Oxford: Clarendon Press, 1955) [Translated into Russian (Moscow: Fizmatgiz, 1959)]
21. van Goor F A et al. *J. Russ. Laser Res.* **18** 247 (1997)
22. Brodskaya B Kh *Khim. Vys. Energ.* **16** 458 (1982)